ELSEVIER

Journal of Alloys and Compounds 434–435 (2007) 565–568

Journal of ALLOYS AND COMPOUNDS

www.elsevier.com/locate/jallcom

The quantum mechanical description of the dot–dot interaction in ionic colloids

P.C. Morais [a,*], Fanyao Qu [b]

[a] *Universidade de Brasília, Instituto de Física, Núcleo de Física Aplicada, 70910-900 Brasília-DF, Brazil*
[b] *Universidade Federal de Uberlândia, Faculdade de Física, 38400-902 Uberlândia-MG, Brazil*

Available online 11 October 2006

Abstract

In this study the dot–dot interaction in ionic colloids is systematically investigated by self-consistently solving the coupled Schrödinger and Poisson equations in the frame of finite difference method (FDM). In a first approximation the interacting two-dot system (dimer) is described using the picture of two coupled quantum wells. It was found that the dot–dot interaction changes the colloid characteristic by changing the hopping coefficient (t) and consequently the nanodot surface charge density (σ). The hopping coefficient and the surface charge density were investigated as a function of the dot size and dot–dot distance.

Keywords: Dot–dot interaction; Ionic colloids; Colloidal stability

1. Introduction

The material system consisting of metal-oxide (M_xO_y) nanodots dispersed in low or high-pH aqueous media is currently named ionic colloid. The ionic magnetic fluid (MF) is a very special class of ionic colloid, where the suspended dot holds a permanent magnetic moment [1]. Colloidal stability is probably one of the finest properties of MFs, which results from a delicate balance between attractive and repulsive dot–dot interaction [2]. Nevertheless, little has been done to understand the fundamental aspects related to colloidal stability outside the classical point of view [3]. In particular, the problem of charge and discharge the suspended dot in a controlled way is an open question [4]. Very recently, however, a proton-tunneling mechanism across the dot–electrolyte interface has been successfully used as a quantum-model picture to calculate the energy levels [5] and the surface charge density [6] in isolated (monomer) M_xO_y semiconductor dots dispersed as ionic colloids. Excellent results for the pH dependence of the surface charge density were obtained from such a quantum-model picture [7,8]. However, as colloidal magnetic dots can be brought close together, for instance, by increasing the dot concentration in the ionic colloid [9] or alternatively by applying external magnetic fields [10], dot–dot coupling in a two-dot system (dimer) may induce remarkable changes on the colloidal characteristic. This issue has never been addressed from the quantum-mechanical viewpoint. In this study, the effects of the coupling between two colloidal dots (dimer) upon the hopping coefficient (t) and surface charge density (σ), driven by differences in dot diameter ($2L_W$) and dot-to-dot distance (b), are theoretically investigated.

2. Problem formulation

Most of the metal-oxide dots used to produce magnetic and non-magnetic ionic colloids are typical semiconductors and so the schematic energy-band diagram proposed for an isolated, spherical M_xO_y quantum dot (QD), immersed in alkaline aqueous solution (negatively charged dot), is represented in Fig. 1. The diagram shown in Fig. 1 resembles the conduction band profile of the well known modulation-doped semiconductor heterostructure [11]. Note that in the chemical synthesis route of magnetic metal-oxide QDs in alkaline medium the precipitated nanodot is negatively charged [12]. The negative charge developed in a metal-oxide nanodot is assumed to be due to partially bonded oxygen atoms ($M_{(s)}$–O^-), where $M_{(s)}$ stands for metal at the dot surface [13]. Neutral hydroxyl group bonded at the dot surface ($M_{(s)}$–OH) also plays a very important role in the chemical equilibrium involving the positively and negatively charged dots [14]. In addition, it will be assumed here that negative charge

* Corresponding author. Tel.: +55 61 32736655; fax: +55 61 32723151.
E-mail address: pcmor@unb.br (P.C. Morais).

0925-8388/$ – see front matter © 2006 Elsevier B.V. All rights reserved.
doi:10.1016/j.jallcom.2006.08.184

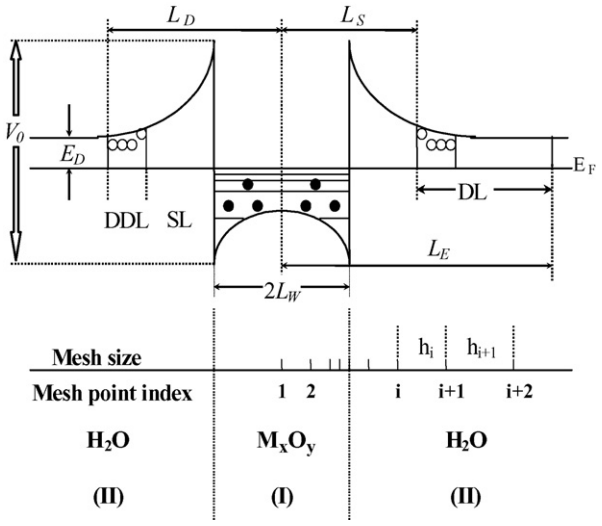

Fig. 1. Schematic energy-band diagram for an M_xO_y/H_2O quantum dot. The discretization of the potential based on a non-uniform mesh is schematically represented as well.

is built up at the aqueous dispersed dot due to proton (H^+) transfer out from the dot surface towards the solvent. Thus, starting at the zero point of charge and increasing the pH value in the aqueous medium the chemisorbed protons (H^+) are assumed to jump out from the dot surface ($M_{(s)}$–OH), leaving behind electrons in the partially bonded oxygen atoms ($M_{(s)}$–O^-). The electron left behind is assumed to be accommodated in the dot conduction band whereas the surface oxygen atoms would be stabilized by a strongly bonded water-layer around the dot surface. Experimental evidence of a thin water-layer strongly bonded at the dot surface in ionic magnetic fluids has been recently obtained from Raman experiments [15]. This proton transfer mechanism sets in a negative surface charge density. In contrast, starting at the zero point of charge and lowering the pH in the aqueous medium the available protons (H^+) are assumed to transfer from the acid solvent back to the dot surface, thus setting up a positive charge on the dot surface ($M_{(s)}$–OH_2^+) [15]. One point, however, deserves special attention, namely, the typical value of the effective mass of the carrier in the barrier ($m_B = 140$). Such a huge effective mass corresponds to the proton (H^+) which transfers into the QD and out from the QD towards the solvent through the strongly bonded water-layer of thickness ($L_S - L_W$). As shown in Fig. 1 the dot diameter is given by $2L_W$, the spacer layer (SL) thickness is ($L_S - L_W$), the donor depletion layer (DDL) thickness is ($L_D - L_S$), and the donor layer (DL) thickness is ($L_E - L_S$). The confined bound states inside the dot are described by $E_{n,l}$ (n, $l = 0, 1, 2, \ldots$). E_D is the donor ionization energy and V_0 is the band offset. In aqueous charged colloids the SL is typically one nanometer thick and is assumed to be due to water molecules strongly bonded at the dot surface. In alkaline aqueous colloids the DDL about the dot corresponds to the region where the positively charged counterions are distributed [16]. Experimental data obtained from M_xO_y semiconductors in aqueous media indicates that V_0 goes up to 1 eV [16], being very sensitive to the pH value [17]. The M_xO_y dot dispersed in water solution is now treated as a spherically symmetric modulation-doped M_xO_y/H_2O quantum dot. The QD electronic structure can be obtained numerically by solving self-consistently the Schrödinger and Poisson's equations in the frame of the FDM with a non-uniform mesh size, as indicated by the mesh point index (see Fig. 1). A successful approach to the solution of the Schrödinger's equation has been the FDM in which real space is divided into discrete mesh points and the wave function (Ψ) is solved within those discrete spacing [18].

3. Results and discussion

Within the frame of the FDM energy levels (E) and wave functions (Ψ) associated to the two-dot system (dimer) are obtained by self-consistently solving the Schrödinger equation:

$$-\frac{\hbar^2\nabla^2}{2m}\Psi + [V_b(z - z_1) + V_b(z - z_2) + V_H]\Psi = E\Psi \quad (1)$$

coupled to the Poisson equation:

$$\varepsilon\frac{d^2V_H}{dx^2} = \frac{e^2[N_D - n(z)]}{\varepsilon_0}, \quad (2)$$

where

$$V_b(z - z_i) = \begin{cases} 0 & |z - z_i| \geq D/2 \\ -V_0 & |z - z_i| \leq D/2 \end{cases}. \quad (3)$$

From Eq. (1) through Eq. (3) $i = 1, 2$, z_1, and z_2 are the two dot positions, and N_D describes the proton (H^+) or hydroxyl (OH^-) concentration in the aqueous medium at low or high pH, respectively. The surface charge density (σ) in the dimer can be obtained by summing over all states:

$$\sigma = \sum_n \frac{m}{\pi\hbar^2}kT\ \ln\{1 + \exp\{[E_F - E_n]/kT\}\}, \quad (4)$$

where k is the Bolzmann constant and T is the absolute temperature. In addition, the tunneling parameter, called here hopping coefficient, is defined as $t = (E_A - E_B)$—energy splitting between the lowest anti-bonding ($|A\rangle$) and bonding ($|B\rangle$) states and calculated by the following transfer integrals:

$$t = \langle\Psi(z - z_1)|V_b(z - z_1)|\Psi(z - z_2)\rangle \quad (5)$$

or

$$t = \langle\Psi(z - z_2)|V_b(z - z_2)|\Psi(z - z_1)\rangle\,, \quad (6)$$

where E_A and E_B are the energy eigenvalues of $|A\rangle$ and $|B\rangle$, respectively.

Numerical calculation was performed for negatively charged (alkaline medium) M_xO_y/H_2O dots. Besides dot–dot distance, dot interaction depends upon the dot diameter, conduction band offset at pH 7, and pH value. At higher or lower pHs, however, band bending occurs due to the built-in surface charge density. The pH value will affect the built-in electric field [6–8] and hence the band bending [19]. Therefore, at least four factors (b, L_W, V_0, and pH) will influence the confinement energy level and surface charge density and thus dot interaction. The following parameters were used in the calculation: room temperature, donor binding energy at 50 meV, L_S equals to 10 Å, m

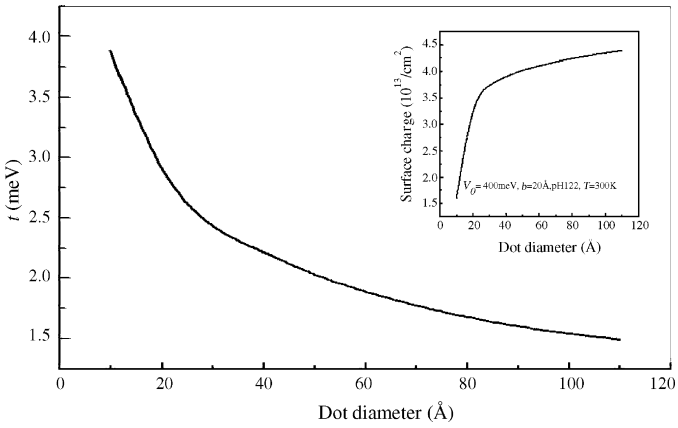

Fig. 2. Hopping coefficient vs. dot diameter, for $V_0 = 400$ meV, $b = 20$ Å, and pH 12.2. Calculation was performed considering the first pair of anti-bonding ($|A\rangle$) and bonding ($|B\rangle$) states, at room temperature. The inset shows the corresponding surface charge density vs. dot diameter.

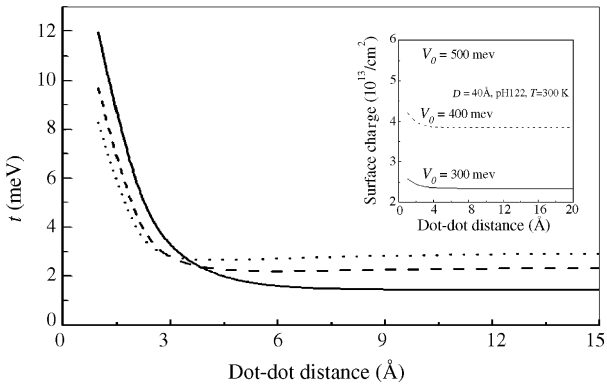

Fig. 3. Hopping coefficient vs. dot–dot distance, for $V_0 = 300$ (solid line), 400 (dashed line), and 500 meV (dotted line). Calculation was performed using $2L_W = D = 40$ Å, pH 12.2, room temperature, and the first pair of anti-bonding ($|A\rangle$) and bonding ($|B\rangle$) states. The inset shows the corresponding surface charge density vs. dot–dot distance.

in the $M_xO_y(H_2O)$ equals to 0.24(140), and ε in the $M_xO_y(H_2O)$ equals to 3.7(80).

Fig. 2 shows the hopping coefficient (t) associated to $|A\rangle$ and $|B\rangle$ whereas the inset shows the corresponding surface charge density as a function of dot diameter, in the range of 10–110 Å, for $V_0 = 400$ meV, $b = 20$ Å, and pH 12.2. It is found that the hopping coefficient reduces monotonically as the dot diameter increases. As the dot diameter decreases, from very large values to about 120 Å, the surface charge density changes very slowly and so the hopping coefficient (see Fig. 2). However, with further decreasing in dot diameter a strong surface discharge process is observed (see Fig. 2). The surface charge density quickly decreases as the dot diameter goes below 30 Å, due to the leaking of the carrier wavefunction out from the dot core region. This means that the tunneling effect becomes very strong for very small dots. Note that the carrier energy levels of an individual dot (monomer), having two-fold degeneracy, splits into a pair of states as dots are brought close together. Thus, the wavefunction of the dimer can be approximated by a linear combination of wavefunctions of monomers. These wavefunctions (Ψ_B and Ψ_A) correspond to bonding and anti-bonding states. Then, in ionic aqueous-based colloids dimers ("artificial molecules") tend to be built spontaneously from monomers ("artificial atoms") as the dot size is reduced. In other words, concentrated ionic aqueous-based magnetic fluids containing very small dots would hardly reach colloidal stability.

Dot–dot distance (surface-to-surface) and band offset values also play a key role in determining the energy level position. Fig. 3 shows t associated to the lowest $|A\rangle$ and $|B\rangle$ states versus b, for $2L_W = 40$ Å, pH 12.2, at three band offset values. The inset of Fig. 3 shows the corresponding surface charge density versus dot–dot distance, for $2L_W = 40$ Å, pH 12.2, at $V_0 = 300$, 400, and 500 meV. Note that dot–dot interaction, which is described through the transfer integral, is strongly dependent upon the potential energy V_0 and dot–dot distance b. For $b > 6$ Å the transfer integral t increases as V_0 increases. On the other hand, b affects the hopping coefficient as a result of the overlap between wave functions of individual dots, which reflects the coupling between dots in the dimer. For large b values the dot–dot coupling is small. However, when dots are brought close together dot–dot coupling gradually increases. Carrier energy levels of individual dots with two-fold degeneracy, prevailing at infinite b, splits into a pair of states. Moreover, by reducing the dot–dot distance between coupled dots the energy splitting and surface charge density increase. Note that the effects introduced by decreasing b are balanced by the effects introduced as V_0 increases. Fig. 3 also revels the crossover among the curves for $V_0 = 300$, 400, and 500 meV at $b = 3.83$, 3.48, and 1.90 Å, respectively. Such crossover is not observed in the absence of a built-in surface charge density.

4. Conclusions

In summary, dot–dot interaction in ionic water-based colloids was studied as a function of dot size and dot–dot distance, taking into account carrier effective masses, dielectric constants, band offset, and pH values by self-consistent calculation of the coupled Schrödinger and Poisson equations. Though approximate the calculation based on two coupled quantum wells can be easily performed within the finite difference method (FDM), allowing important conclusions regarding colloid stability. It is found from the calculations based on FDM that colloidal stability in ionic magnetic fluids is extremely dependent upon intrinsic parameters (dot size and band offset values) and extrinsic parameters (dot concentration and pH values).

Acknowledgments

This work was partially supported by the Brazilian agencies FINATEC, FAPEMIG, and CNPq.

References

[1] P.C. Morais, V.K. Garg, A.C. Oliveira, L.P. Silva, R.B. Azevedo, A.M.L. Silva, E.C.D. Lima, J. Magn. Magn. Mater. 225 (2001) 37–40.
[2] N. Buske, Prog. Colloid Polym. Sci. 95 (1994) 175–180.
[3] G.M. Bell, S. Levine, L.N. McCartney, J. Colloid Interface Sci. 33 (1970) 335–359.
[4] M. Chen, W. Porod, J. Appl. Phys. 78 (1995) 1050–1057.

[5] Fanyao Qu, P.C. Morais, J. Chem. Phys. 111 (1999) 8588–8594.
[6] Fanyao Qu, P.C. Morais, J. Phys. Chem. B 104 (2000) 5232–5236.
[7] Fanyao Qu, P.C. Morais, IEEE Trans. Magn. 37 (2001) 2654–2656.
[8] Fanyao Qu, P.C. Morais, J. Magn. Magn. Mater. 252 (2002) 117–119.
[9] K. Skeff Neto, A.F. Bakuzis, P.C. Morais, A.R. Pereira, R.B. Azevedo, L.M. Lacava, Z.G.M. Lacava, J. Appl. Phys. 89 (2001) 3362–3369.
[10] K.T. Wu, Y.D. Yao, H.K. Huang, J. Magn. Magn. Mater. 209 (2000) 246–248.
[11] Y.-H. Zhang, R. Cingolani, K. Ploog, Phys. Rev. B 44 (1991) 5958–5961.
[12] R. Massart, IEEE Trans. Magn. 17 (1981) 1247–1248.
[13] H. Herrmann, S.T. Martin, M.R. Hoffmann, J. Phys. Chem. 99 (1995) 16641–16645.
[14] L.X. Chen, T. Rajh, Z. Wang, M.C. Thurnauer, J. Phys. Chem. B 101 (1997) 10688–10697.
[15] A.W. Adamson, Physical Chemistry of Surfaces, John Wiley, New York, 1990.
[16] (a) B. O'Regan, J. Moser, M. Anderson, M. Grätzel, J. Phys. Chem. 94 (1990) 8720–8726;
(b) G. Rothenberg, D. Fitzmaurice, M. Grätzel, J. Phys. Chem. 96 (1992) 5983–5986.
[17] R. Hoyle, J. Sotomayor, G. Will, D. Fitzmaurice, J. Phys. Chem. 101 (1997) 10791–10800.
[18] I.-H. Tan, G.L. Snider, L.D. Chang, E.L. Hu, J. Appl. Phys. 68 (1990) 4071–4076.
[19] Fanyao Qu, P.C. Morais, IEEE J. Quantum Electron. 34 (1998) 1419–1425.